

Investigation of actuation voltage for non-uniform serpentine flexure design of RF-MEMS switch

Ashish Kumar Sharma · Navneet Gupta

Received: 10 April 2013 / Accepted: 27 September 2013 / Published online: 13 October 2013
© Springer-Verlag Berlin Heidelberg 2013

Abstract This paper presents an attempt to reduce the actuation voltage of capacitive RF-MEMS switch by introducing the concept of non-uniform serpentine flexure suspensions. The spring constant of non-uniform serpentine flexure with different meander sections have been equated by analytical expression and verified with finite element method (FEM). FEM analysis indicate actuation voltage as low as 5 V with single meander section for the proposed non-uniform serpentine spring design, which is reasonably low as compared to uniform serpentine spring with same span beam length.

1 Introduction

Radio-frequency micro electro mechanical systems (RF-MEMS) technology offers a great future of RF component such as RF-MEMS switches for wireless communication. These RF-MEMS switches are the prime candidate in RF and microwave communication systems as compared to solid state switches because they exhibit low power consumption, low insertion loss, high isolation with high RF power handling capabilities (Balaraman et al. 2002; Goldsmith et al. 1995; Jensen et al. 2003; Yao and Chang 1995). Several researchers have proposed various designs of capacitive RF-MEMS switches to overcome the high actuation voltage requirements (Yao and Chang 1995; Pacheco et al. 1998; Rizk 2000). The use of serpentine

suspensions with higher meander sections have been used to achieve lower actuation voltage, which often compromise with space limitation and design complexity (Pacheco et al. 2000). The push pull concept and electromagnetic actuation mechanism have also been proposed to reduce the actuation voltage (Hah et al. 2000). RF-MEMS switches with two actuation mechanism have also been demonstrated but these switches were not used in RF and microwave devices due to their complicated fabrication process with a major challenge of residual stress control (Cho et al. 2005). In addition, recently a new design using a freely moving contact pad has been elaborated but this design suffers with serious limitation of operating angle range, which increases the actuation voltage requirement (Lee et al. 2006). In this paper a simple and effective design concept of non-uniform serpentine flexure suspension has been introduced which lowers the spring constant and actuation voltage.

2 Mechanical design of capacitive RF-MEMS switch

This section describes the actuation voltage calculation for non-uniform serpentine flexure based RF-MEMS switch. This switch beam is suspended at a height of g_0 above the dielectric layer on the transmission line as shown in Fig. 1. The actuation voltage for fixed-fixed capacitive RF-MEMS switch can be given as (Rebeiz 2003)

$$V_p = \sqrt{\frac{8K_z}{27\varepsilon_0 Ww}} g_0^3 \quad (1)$$

where W is the width of the actuation electrode, w is the width of bridge structure, ε_0 is the permittivity of free space, K_z is total spring constant for RF-MEMS switch and g_0 is the initial gap between the electrode and MEMS bridge with zero potential.

A. K. Sharma · N. Gupta (✉)
Department of Electrical and Electronics Engineering,
Birla Institute of Technology and Science,
Pilani 333 031, Rajasthan, India
e-mail: dr.guptanavneet@gmail.com;
ngupta@pilani.bits-pilani.ac.in

A. K. Sharma
e-mail: ashish.sharma@pilani.bits-pilani.ac.in

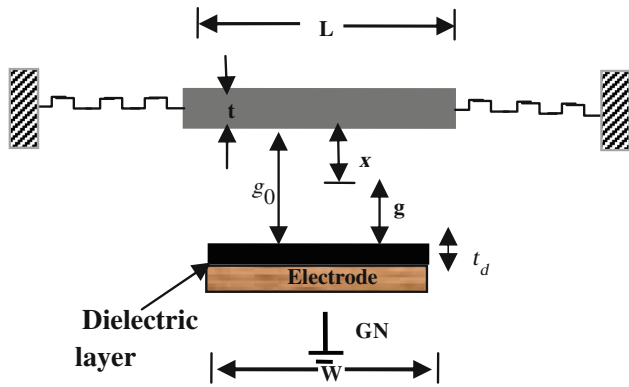


Fig. 1 Sketch of a fixed–fixed beam capacitive RF-MEMS switch

So this total spring constant (K_z) will be the sum of all four serpentine spring attached to the flexure, which can be given as:

$$K_z = \frac{4k_z}{N} \tag{2}$$

where k_z is the spring constant for single spring and N is the number of meander sections. From Eq. 1, it is clear that the actuation voltage can be reduced in three different ways: first by decreasing the height between the bridge and the electrode, secondly by increasing the area of the bridge and lastly diminishing the bridge structure with low spring constant. Out of these possibilities, the third possibility depends on spring constant K_z . So actuation voltage can be minimized by using a serpentine spring with less K_z . So we propose a non-uniform serpentine spring design to reduce the spring constant of RF-MEMS switches.

3 Non-uniform serpentine flexure design

A schematic of non-uniform serpentine spring with two meander sections is shown in Fig. 2a. Each meander is made of four beam segments, called as connector beams and span beams. These connector beams and span beams are denoted as meander length and meander width with the length of a and b respectively. These beams are having the thickness of t and width of w' . For non-uniform serpentine flexure design the meander width (b) increases in multiples of varying span beam segments. Here for two meander sections for four span beams the meander widths can be represented as $b, 2b, 3b$ and $4b$. Non-uniform serpentine spring get their name due their non-uniform meander width. The meanders width can be adjusted to provide the appropriate stiffness ratio with reduced spring constant (Jaecklin et al. 1993). Most of the uniform serpentine springs are designed with constant meander width (Pacheco et al. 2000; Zhang and MacDonald 1991). These developed micromechanical serpentine spring designs exhibit low

spring constant, which increases the sensitivity to frictional effects of the beam joints (Pisano and Cho 1989). So we propose a varying meander width concept to reduce the spring constant of RF-MEMS switches. Because of 2-fold flexure symmetry of non-uniform serpentine flexure, the spring constant calculation is done for single spring as shown in Fig. 2b. A perpendicular force F_z is applied in z direction at the end of the beam resulting in a displacement of δ_z . We have chosen the z coordinate direction for spring constant calculation. The guided end has separate ε and δ coordinate system where ε is the coordinate along the beam axis and δ is the coordinate normal to the ε axis. Here rotational angle of θ_0 and ϕ_0 are considered from guided end boundary conditions. These boundary end conditions are derived from free body diagram as given for uniform serpentine spring structure (Fedder 1994). Residual stress and extensional stress are neglected in the following analysis. Bending moment and torsion for connector and span beam segments ($i, j = 1-2N$) have been given in Table 1.

The total energy for non-uniform serpentine spring is given by

$$U = \sum_{i=1}^{2N} \int_0^a \left(\frac{M_{a,i}^2}{2EI_{x,a}} + \frac{T_{a,i}^2}{2GJ_a} \right) d\varepsilon + \sum_{j=1}^{2N} \int_0^b \left(\frac{M_{b,j}^2}{2EI_{x,b}} + \frac{T_{b,j}^2}{2GJ_b} \right) d\varepsilon \tag{3}$$

where E is the Young’s Modulus of elasticity, G is the torsion (or shear) modulus of the elasticity, J is the torsion constant, $I_{x,a}$ and $I_{x,b}$ are the bending moment of inertia about x axis for connector and span beam segments respectively. The guided end constraints tilt θ_0 and rotation ϕ_0 at the end of connector beam segment can be written as follows

$$\begin{aligned} \theta_0 &= \frac{\partial U}{\partial M_0} \\ &= \sum_{i=1}^{2N} \int_0^a \left(\frac{M_{a,i}}{EI_{x,a}} \frac{\partial M_{a,i}}{\partial M_0} + \frac{T_{a,i}}{GJ_a} \frac{\partial T_{a,i}}{\partial M_0} \right) d\varepsilon \\ &\quad + \sum_{j=1}^{2N} \int_0^b \left(\frac{M_{b,j}}{EI_{x,b}} \frac{\partial M_{b,j}}{\partial M_0} + \frac{T_{b,j}}{GJ_b} \frac{\partial T_{b,j}}{\partial M_0} \right) d\varepsilon \\ &= 0 \end{aligned} \tag{4}$$

$$\begin{aligned} \phi_0 &= \frac{\partial U}{\partial T_0} \\ &= \sum_{i=1}^{2N} \int_0^a \left(\frac{M_{a,i}}{EI_{x,a}} \frac{\partial M_{a,i}}{\partial T_0} + \frac{T_{a,i}}{GJ_a} \frac{\partial T_{a,i}}{\partial T_0} \right) d\varepsilon \\ &\quad + \sum_{j=1}^{2N} \int_0^b \left(\frac{M_{b,j}}{EI_{x,b}} \frac{\partial M_{b,j}}{\partial T_0} + \frac{T_{b,j}}{GJ_b} \frac{\partial T_{b,j}}{\partial T_0} \right) d\varepsilon \\ &= 0 \end{aligned} \tag{5}$$

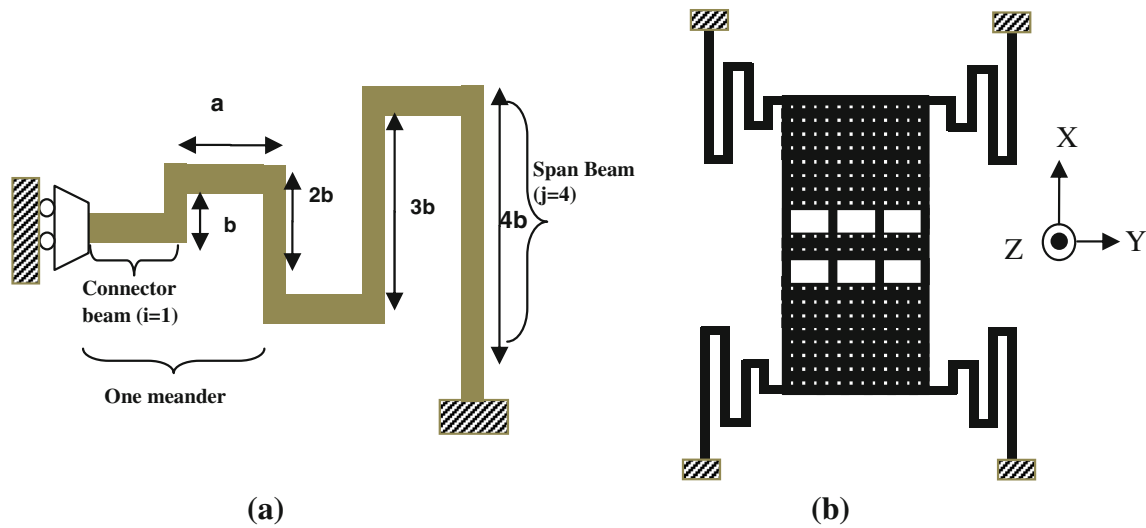


Fig. 2 **a** Schematic of non-uniform serpentine flexure with two meander sections. **b** RF-MEMS switch beam with non-uniform serpentine flexure

Table 1 Bending moment and torsion for connector and span beam segments for two meander sections ($N = 2$)

Connector beam segments ($i = 1-2N$)		Span beam ($j = 1-2N$)	
Bending moment ($M_{a,i}$)	Torsion ($T_{a,i}$)	Bending moment ($M_{b,j}$)	Torsion ($T_{b,i}$)
$M_{a,1} = M_o - F_z \epsilon$	$T_{a,1} = T_o$	$M_{b,1} = -T_o - F_z \epsilon$	$T_{b,1} = M_o - F_z \epsilon$
$M_{a,2} = M_o - F_z \epsilon - F_z a$	$T_{a,2} = -(-T_o - F_z b) = T_o + F_z b$	$M_{b,2} = T_o + F_z b - F_z \epsilon$	$T_{b,2} = -M_o + 2F_z a$
$M_{a,3} = M_o - 2F_z a - F_z \epsilon$	$T_{a,3} = T_o + F_z b - F_z 2b = T_o - F_z b$	$M_{b,3} = -T_o + F_z b - F_z \epsilon$	$T_{b,3} = M_o - 3F_z a$
$M_{a,4} = M_o - 3F_z a - F_z \epsilon$	$T_{a,4} = -(-T_o + F_z b - F_z 3b) = T_o + 2F_z b$	$M_{b,4} = T_o + 2F_z b - F_z \epsilon$	$T_{b,4} = -M_o + 4F_z a$

The moment and torsion of each beam segment will be calculated as a function of position along the beam’s z axis. We can calculate the resulting moment and torsion for applied unit load at beam segments.

$$M_0 = F_z \left(\frac{G.J8a^2 + EI_x 30ab}{G.J4a + EI_x 10b} \right) = F_z C_1 \tag{6}$$

$$T_0 = -F_z \left(\frac{G.J7b^2 + EI_x 2ab}{G.J10b + EI_x 4a} \right) = -F_z C_2 \tag{7}$$

where $C_1 = \frac{G.J8a^2 + EI_x 30ab}{G.J4a + EI_x 10b}$ and $C_2 = \frac{G.J7b^2 + EI_x 2ab}{G.J10b + EI_x 4a}$ are the constants, used to simplify the mathematical calculations. Now we substitute M_0 and T_0 in the equations of bending moment and torsion of connector and span beam segments (Table 1). Now these new equations of bending moment and torsion will be used to obtain the vertical displacement of the serpentine spring in z direction. The unit load method (Castigliano’s second theorem) is employed to determine the deflection of the beam (Timoshenko and Goodier 1970).

Table 2 RF-MEMS switch design parameters

Parameter name	Parameter values
Span beam length (b)	100–280 μm
Connector beam length (a)	25 μm
Span and connector beam thickness (t)	1.5 μm
Ni Young’s Modulus of beam material (E)	207 GPa
Density of nickel (Ni)	8.9 g/cm^3
Inertia about x axis (I_x)	$I_x = wr^3/12$
Torsion modulus of the elasticity (G)	$G = E/(2(1 + \nu))$
Inertia about z axis (I_z)	$I_z = tw^3/12$
Span and connector beam width (w')	10 μm
Poisson’s ratio (ν)	0.31
Width of beam structure (w)	104 μm
Switch beam length (L)	640 μm
Gap height (g_o)	3 μm
Switch beam thickness (t)	1.5 μm
Electrode width (W)	100 μm
Torsion constant (J)	$J = 0.413 (I_x + I_z)$

Fig. 3 Comparison of analytically calculated spring constant with FEM simulated values for non-uniform serpentine spring with different span beam lengths (b) ranges from 100 to 280 μm , with one meander section

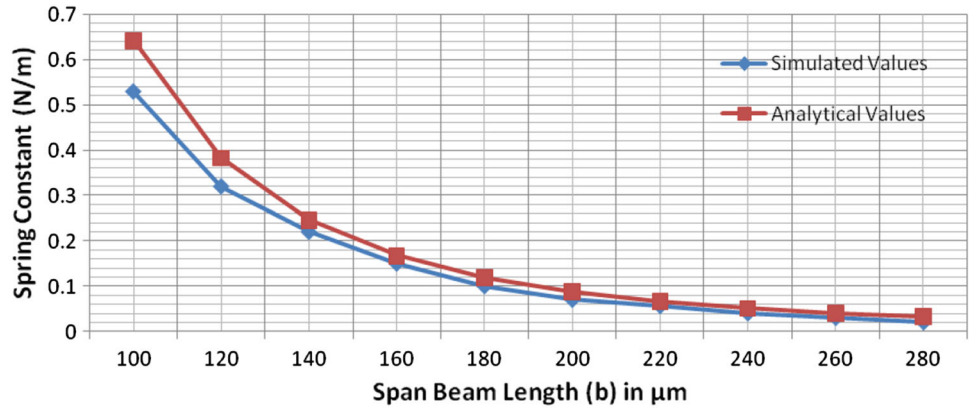


Fig. 4 Actuation voltage comparison between uniform and non-uniform serpentine flexure based RF-MEMS switch, with different span beam lengths (b) ranges from 100 to 280 μm , with one meander section

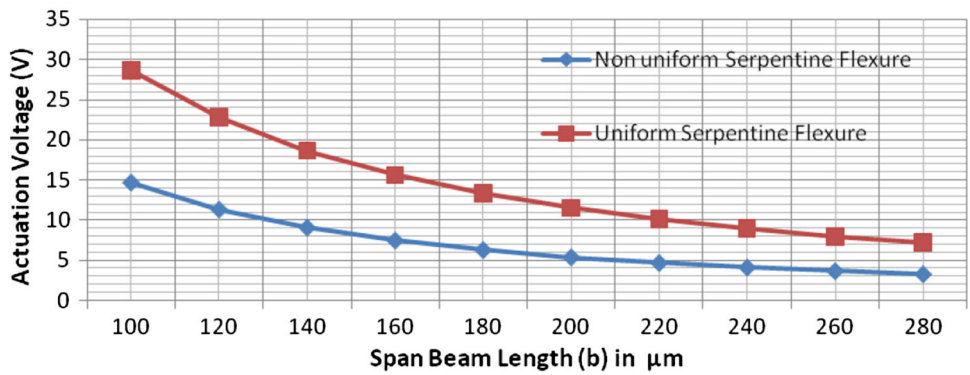
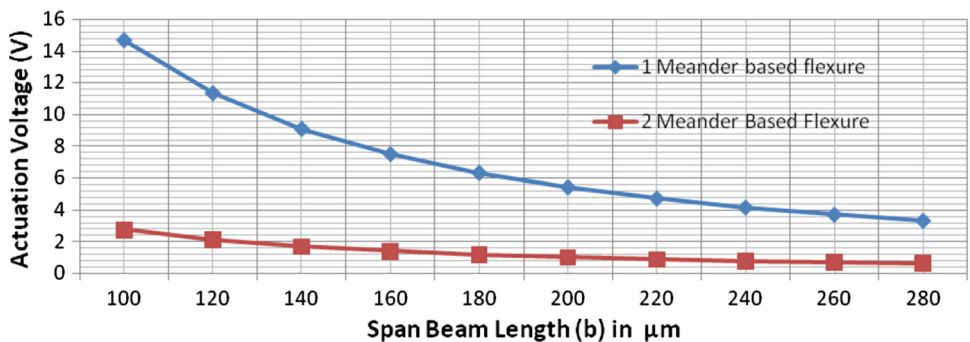


Fig. 5 Actuation voltage comparison between one and two meander based RF-MEMS switch, with different span beam lengths (b) ranges from 100 to 280 μm



$$\begin{aligned} \delta_z &= \frac{\partial U}{\partial F_z} \\ &= \sum_{i=1}^{2N} \int_0^a \left(\frac{M_{a,i}}{EI_{x,a}} \frac{\partial M_{a,i}}{\partial F_z} + \frac{T_{a,i}}{GJ_a} \frac{\partial T_{a,i}}{\partial F_z} \right) d\varepsilon \\ &\quad + \sum_{j=1}^{2N} \int_0^{jb} \left(\frac{M_{b,j}}{EI_{x,b}} \frac{\partial M_{b,i}}{\partial F_z} + \frac{T_{b,j}}{GJ_b} \frac{\partial T_{b,i}}{\partial F_z} \right) d\varepsilon \end{aligned} \tag{8}$$

We can simplify this equation for beam displacement as follows:

$$\delta_z = \delta_{z1} + \delta_{z2} + \delta_{z3} + \delta_{z4} \tag{9}$$

where $\delta_{z1} = \sum_{i=1}^{2N} \int_0^a \left(\frac{M_{a,i}}{EI_{x,a}} \frac{\partial M_{a,i}}{\partial F_z} \right) d\varepsilon$, $\delta_{z2} = \sum_{i=1}^{2N} \int_0^a \left(\frac{T_{a,i}}{GJ_a} \frac{\partial T_{a,i}}{\partial F_z} \right) d\varepsilon$, $\delta_{z3} = \sum_{j=1}^{2N} \int_0^{jb} \left(\frac{M_{b,j}}{EI_{x,b}} \frac{\partial M_{b,i}}{\partial F_z} \right) d\varepsilon$ and $\delta_{z4} = \sum_{j=1}^{2N} \int_0^{jb} \left(\frac{T_{b,j}}{GJ_b} \frac{\partial T_{b,i}}{\partial F_z} \right) d\varepsilon$

are the displacements for connector and span beam segments because of the bending moment and torsion. The z direction spring constant for two meander based non-uniform spring can be given as:

$$k_z = \frac{F_z}{\delta_{z1} + \delta_{z2} + \delta_{z3} + \delta_{z4}} \tag{10}$$

$$\begin{aligned} k_z &= \left[\frac{1}{EI_{x,a}} \left(4C_1^2 a + \frac{64}{3} a^3 - 16C_1 a^2 + 10C_2^2 b - 24b^3 + \frac{100}{3} b^3 \right) \right. \\ &\quad \left. + \frac{1}{GJ_a} (4C_2^2 a + 6b^2 a - 4C_2 b a + 10C_1^2 b + 100a^2 b - 60C_1 a b) \right]^{-1} \end{aligned} \tag{11}$$

Equation 11 shows the spring constant for two meander based non-uniform serpentine spring. Now this spring constant analysis can also be used to determine the spring

constant for different meander based non-uniform serpentine flexures.

4 Results and discussion

Table 2 shows the parameters used for calculating the spring constant and actuation voltage of non-uniform serpentine flexure for RF-MEMS switch. Analytically calculated spring constant is verified by finite element method analysis (FEM). These dimensions of non-uniform serpentine spring were applied to FEM simulation tool (COMSOL Multiphysics version 4.2, <http://www.comsol.com/sla>) and these results are compared with analytical calculation. We applied a concentrated z direction force of $1 \mu\text{N}$ at the free end of the non-uniform serpentine spring, which produces the beam displacement of (δ_z). Here we observed that analytically calculated spring constant is 1–2 % higher than the simulated values due to the absence of residual stress as shown in Fig. 3. This figure also signifies a close agreement between analytical and simulated values of spring constant for single meander non-uniform serpentine flexure. This spring constant analysis is used to achieve low actuation voltage for non-uniform serpentine flexure based RF-MEMS switch. Here the maximum span beam length is restricted only up to $280 \mu\text{m}$ in order to remove the possibility of system complexity, which may arise due to increase in overall size of the switch. Figure 4 compare the actuation voltage of uniform and non-uniform serpentine flexure based RF-MEMS switches for similar values of span beam length. This plot illustrate that non-uniform serpentine flexure provides actuation voltage of 15–3 V for span beam length from 100 to $280 \mu\text{m}$. But the uniform serpentine flexure provides an actuation voltage of 28–8 V for the same span beam lengths (Peroulis 2003). It is also observed that the actuation voltage decreases rapidly for span beam length 100– $180 \mu\text{m}$ but the curve is almost linear from 200 to $280 \mu\text{m}$. So the use of span beam with more than $200 \mu\text{m}$ is not a good decision because it increases flexure's dimension without affecting the actuation voltage much. Figure 5 illustrates that actuation voltage can be reduced further by increasing the number of meander sections. Here it is not recommended to use more than one meander sections because it will lead to structure complexity with space limitations for RF applications. Hence, it is confirmed that non-uniform serpentine flexure with $200 \mu\text{m}$ span beam length with single meander section would be a good decision in order to produce an actuation voltage of 5 V.

5 Conclusion

A non-uniform serpentine flexure design for RF-MEMS switch has been proposed in this paper. This non-uniform serpentine flexure uses a varying span beam length, which results in varying meander width with reduced spring constant. This reduced spring constant is used to achieve low actuation voltage for RF-MEMS switches. RF-MEMS switch with single meander section using a non-uniform serpentine flexure with $200 \mu\text{m}$ span beam length, offers an actuation voltage of 5 V. This obtained actuation voltage is significantly lower than a RF-MEMS switch using a uniform serpentine flexure with same meander dimensions. Here we also observed that this actuation voltage can further be reduced by using two meander sections with non-uniform serpentine flexure; however it leads with more structure complexity with space limitations.

Acknowledgments The authors would like to thank NNMDC Lab BITS Pilani, Rajasthan, India, for simulation work.

References

- Balaraman D, Bhattacharya SK, Ayazi F, Papapolymerou J (2002) Low-cost low actuation voltage copper RF-MEMS switches. *IEEE Microw Theory Tech Symp* 2:1225–1228
- Cho II-J, Song T, Baek S-H, Yoon E (2005) Low voltage and low power RF MEMS series and shunt switches actuated by combination of electromagnetic and electrostatic forces. *IEEE Trans Microw Theory Tech* 53:2450–2457
- Fedder GK (1994) Simulation of microelectromechanical systems. Phd dissertation, Electrical Engineering and Computer Science, University of California
- Goldsmith C, Lin T-H, Powers B, Wu W-R, Norvell B (1995) Micromechanical membrane switches for microwave applications. *IEEE Microw Theory Tech Symp* 1:91–94
- Hah D, Yoon E, Hong S (2000) A low voltage actuated micromachined microwave switch using torsion springs and leverage. *IEEE Trans Microw Theory Tech* 1:2540–2545
- Jensen BD, Wan Z, Chow L, Saitou K, Kurabayashi K, Volakis JL (2003) Integrated electrothermal modeling of RF-MEMS switches for improved power handling capability. In: *IEEE topical conference on wireless communication technology*, pp 10–11
- Jaecklin VP, Linder C, de Rooij NF (1993) Optical microshutters and torsional micromirrors for light modulator arrays. In: *IEEE micro electro mechanical systems workshop proceedings, Florida, February 1993*, pp 124–127
- Lee S-D, Jun B-C, Kim S-D, Park H-C, Rhee J-K, Mizuno K (2006) An RF-MEMS switch with low-actuation voltage and high reliability. *J Microelectromech Sys* 15:1605–1611
- Peroulis D (2003) RF-MEMS devices for multifunctional integrated circuits and antennas. Phd thesis, The University of Michigan
- Pacheco S, Nguyen C-T, Katehi LPB (1998) Micromechanical electrostatic K-band switches. *IEEE Microw Theory Tech Symp* 3:1569–1572
- Pacheco S, Nguyen C-T, Katehi LPB (2000) Design of low actuation voltage RF MEMS switch. *IEEE Microw Theory Tech Symp* 1:165–168

- Pisano AP, Cho Y-H (1989) Mechanical design issues in laterally-driven microstructures. In: 5th international conference on solid-state sensors and actuators technical digest, Switzerland, June 1989, pp 1060–1064
- Rizk JB, Muldavin JB, Tan G-L, Rebeiz GM (2000) Design of X-band MEMS microstrip shunt switches. In: 30th European microwave conference, 2000, pp 1–4
- Rebeiz GM (2003) RF MEMS: theory, design, and technology, 3rd edn. John Wiley, New Jersey
- Timoshenko SP, Goodier JN (1970) Theory of elasticity, 3rd edn. McGraw-Hill, New York
- Yao JJ, Chang MF (1995) A surface micro machined miniature switch for telecommunications applications with signal frequencies from dc up to 4 ghz. In: The 8th international conference on solid-state sensors and actuators, and Eurosensors IX, Stockholm, June 1995, pp 384–387
- Zhang ZL, MacDonald N (1991) An Rie process for submicron, silicon electromechanical structures in technical digest. In: 6th international conference on solid-state sensors and actuators, 1991, pp 520–523